Anal. Chem. **2010,** *82,* 2803–2810

Controlled and Efficient Hybridization Achieved with DNA Probes Immobilized Solely through Preferential DNA-Substrate Interactions

Sarah M. Schreiner,[†] David F. Shudy,[†] Anna L. Hatch,[†] and Aric Opdahl*[,†]

Department of Chemistry, University of Wisconsin—La Crosse, La Crosse, Wisconsin 54601

Lloyd J. Whitman[‡,#] and Dmitri Y. Petrovykh*[,‡,§]

Naval Research Laboratory, Washington, DC 20375, and Department of Physics, University of Maryland, College Park, Maryland 20742

Quantitative and reproducible data can be obtained from surface-based DNA sensors if variations in the conformation and surface density of immobilized single-stranded DNA capture probes are minimized. Both the conformation and surface density can be independently and deterministically controlled by taking advantage of the preferential adsorption of adenine nucleotides (dA) on gold, as previously demonstrated using a model system in Opdahl, A.; Petrovykh, D. Y.; Kimura-Suda, H.; Tarlov, M. J.; Whitman, L. J. *Proc. Natl. Acad. Sci. U.S.A.* 2007, 104, 9−14. Here, we describe the immobilization and subsequent hybridization properties of a 15-nucleotide DNA probe sequence that has additional *m* adenine nucleotides, $(dA)_m$, at the 5′ end. Quantitative analysis of immobilization and hybridization for these probes indicates that the $(dA)_m$ block preferentially adsorbs on gold, forcing the probe portion of the strand to adopt an upright conformation suited for efficient hybridization. In addition, a wide range of probe-to-probe lateral spacing can be achieved by coimmobilizing the probe DNA with a lateral spacer, a strand of *k* adenine nucleotides, $(dA)_k$. Altering either the length or relative concentration of the $(dA)_k$ spacers added during probe immobilization controls the average surface density of probes; the density of probes, in turn, systematically modulates their hybridization with solution targets.

Quantitatively correlating the response of DNA sensors to clinically and biologically significant sample abundances requires optimizing the reproducibility of hybridization between DNA targets and surface-bound DNA probes.[1,2] Although gold surfaces are not used in commercial fluorescence-based DNA arrays, gold offers many useful properties as a model substrate[3] and has been successfully used in systematic studies of the interactions governing DNA hybridization near interfaces.[4−8]

The hybridization behavior of surface-immobilized DNA probes strongly depends on the probe conformation and on the lateral spacing between adjacent probes. Hybridization is generally enhanced for DNA probes that extend away from a surface, in part because steric hindrance is lower for such brushlike probes than for DNA directly adsorbed on gold. At surface densities $\leq 5 \times 10^{12}$ cm^{-2}, typical probe sequences (15−30 nucleotides) can hybridize with efficiencies >60%,[7−10] but at probe densities $>1 \times 10^{13}$ cm^{-2} hybridization efficiency is often reduced because of increased electrostatic repulsion and steric constraints.[11−13]

Surfaces with DNA probes in upright conformations can be prepared following a number of strategies, including adsorption via a thiol incorporated at one end (DNA−SH) or coupling DNA probes to bifunctional monolayers.[4−8,14−18] Preparing DNA probes

* To whom correspondence should be addressed. E-mail: opdahl.aric@uwlax.edu (A.O.); dmitri.petrovykh@nrl.navy.mil (D.Y.P.). Phone: 608-785-8274 (A.O.); 202-404-3381 (D.Y.P.).

† University of Wisconsin—La Crosse.

‡ Naval Research Laboratory.

§ University of Maryland.

Current address: Center for Nanoscale Science and Technology, National Institute of Standards and Technology, Gaithersburg, Maryland 20899.

(1) Levicky, R.; Horgan, A. *Trends Biotechnol.* **2005**, *23*, 143–149.
(2) Draghici, S.; Khatri, P.; Eklund, A. C.; Szallasi, Z. *Trends Genet.* **2006**, *22*, 101–109.
(3) Love, J. C.; Estroff, L. A.; Kriebel, J. K.; Nuzzo, R. G.; Whitesides, G. M. *Chem. Rev. (Washington, DC)* **2005**, *105*, 1103–1169.
(4) Wolf, L. K.; Gao, Y.; Georgiadis, R. M. *Langmuir* **2004**, *20*, 3357–3361.
(5) Levicky, R.; Herne, T. M.; Tarlov, M. J.; Satija, S. K. *J. Am. Chem. Soc.* **1998**, *120*, 9787–9792.
(6) Lee, C. Y.; Gong, P.; Harbers, G. M.; Grainger, D. W.; Castner, D. G.; Gamble, L. J. *Anal. Chem.* **2006**, *78*, 3316–3325.
(7) Gong, P.; Lee, C. Y.; Gamble, L. J.; Castner, D. G.; Grainger, D. W. *Anal. Chem.* **2006**, *78*, 3326–3334.
(8) Herne, T. M.; Tarlov, M. J. *J. Am. Chem. Soc.* **1997**, *119*, 8916–8920.
(9) Steel, A. B.; Herne, T. M.; Tarlov, M. J. *Anal. Chem.* **1998**, *70*, 4670–4677.
(10) Peterson, A. W.; Heaton, R. J.; Georgiadis, R. M. *Nucleic Acids Res.* **2001**, *29*, 5163–5168.
(11) Vainrub, A.; Pettitt, B. M. *Phys. Rev. E* **2002**, *66*, 041905.
(12) Vainrub, A.; Pettitt, B. M. *J. Am. Chem. Soc.* **2003**, *125*, 7798–7799.
(13) Demers, L. M.; Mirkin, C. A.; Mucic, R. C.; Reynolds, R. A.; Letsinger, R. L.; Elghanian, R.; Viswanadham, G. *Anal. Chem.* **2000**, *72*, 5535–5541.
(14) Nelson, B. P.; Grimsrud, T. E.; Liles, M. R.; Goodman, R. M.; Corn, R. M. *Anal. Chem.* **2001**, *73*, 1–7.
(15) De Paul, S. M.; Falconnet, D.; Pasche, S.; Textor, M.; Abel, A. P.; Kauffmann, E.; Liedtke, R.; Ehrat, M. *Anal. Chem.* **2005**, *77*, 5831–5838.
(16) Su, X. D.; Wu, Y. J.; Robelek, R.; Knoll, W. *Langmuir* **2005**, *21*, 348–353.
(17) Lee, C. Y.; Nguyen, P. C. T.; Grainger, D. W.; Gamble, L. J.; Castner, D. G. *Anal. Chem.* **2007**, *79*, 4390–4400.
(18) Petrovykh, D. Y.; Kimura-Suda, H.; Whitman, L. J.; Tarlov, M. J. *J. Am. Chem. Soc.* **2003**, *125*, 5219–5226.

10.1021/ac902765g
Published on Web 03/02/2010

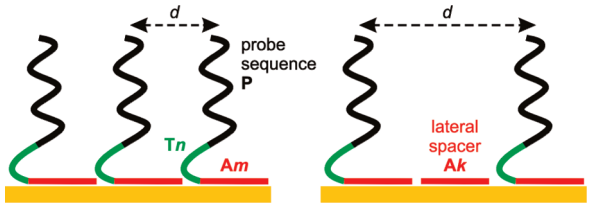

Figure 1. DNA probes immobilized on gold in L-shaped conformation. Preferential adsorption of adenine blocks (A*m*, red) results in a roughly L-shaped conformation of A*m*−T*n*−P strands, where the probe sequence (P, black) is forced into an upright conformation that promotes efficient hybridization. The short block of *n* thymine nucleotides (T*n*, green) serves as a *vertical* spacer. The average spacing, *d*, between adjacent probes is controlled by the length *m* of A*m* attachment blocks (left) or by coimmobilizing A*m*−T*n*−P with adenine strands of length *k* (A*k*), which act as *lateral* spacers (right).

at reproducible surface densities, however, is a critical challenge for common immobilization methods. For example, the surface density and conformation of DNA−SH on gold can be controlled by post-treating DNA-coated surfaces with displacing small thiols, but the kinetics of the displacement reaction vary with the solution and surface conditions, thus limiting reproducibility.

A recently introduced method allows both the conformation and the surface density of DNA probes to be deterministically controlled by taking advantage of an unusually strong interaction between adenine nucleotides (dA) and gold.[19] Nucleotide affinities for gold follow the order A > G ≈ C ≫ T, as demonstrated by competitive adsorption from solution mixtures of homo-oligonucleotides.[20] When blocks of adenine nucleotides are incorporated into a DNA strand, e.g., as a terminal block of a sequence, a similar competition for adsorption sites on gold results in the adenine blocks saturating the surface and forcing the rest of the strand (probe sequence) into an upright conformation (Figure 1). Adjusting the length of adenine blocks controls the footprint of each strand on the surface, thereby deterministically controlling the surface density of probes.[19]

Here, we investigate the practicality of DNA attachment via adenine blocks by immobilizing a DNA probe that includes a mixed 15-nucleotide portion and a terminal block of adenine. Surface plasmon resonance (SPR) imaging spectroscopy and X-ray photoelectron spectroscopy (XPS) provide in situ and ex situ quantitative measurements of surface densities of these DNA probes and of their hybridization properties. We present evidence for both features of the attachment method schematically described in Figure 1: these DNA probes adopt a roughly L-shaped conformation and the average spacing between the A*m*−T*n*−P probes can be controlled by coimmobilizing them with strands of *k* adenine nucleotides (A*k*). We also demonstrate that this DNA immobilization method provides a significant degree of control over reproducibility, hybridization properties, stability, and compatibility with common laboratory procedures.

EXPERIMENTAL DETAILS

Materials. All DNA was obtained from IDT-DNA (Coralville, IA). The 15-nucleotide probe sequence, 5′-CAATGCAGATACACT-3′ (denoted as P15), was chosen to avoid self-hybridization and to minimize formation of secondary structures. This P15 probe sequence was incorporated into several strands having a general "block" structure A*m*−T*n*−P15, where *m* is the number of adenine nucleotides (*m* = 0, 5, 10, 15) and *n* is the number of thymine nucleotides (*n* = 5, 10). The 3′ thiol-modified probe containing the P15 sequence and a five-thymine nucleotide spacer sequence (denoted P15−T5−SH) was used as received without removing the $-S-(CH_2)_3-OH$ protecting group. Additional sequences include the full complement to P15, 5′-AGTGTATCTGCATTG-3′ (denoted P15′), 7-, 15-, and 25-nucleotide adenine oligos (A7, A15, and A25), a 15-nucleotide thymine oligo (T15), and an A15−T20 oligo. Buffers denoted as NaCl-TE and $CaCl_2$-TE contained 1× TE (10 mM Tris·HCl, 1 mM EDTA) with 1 M NaCl or $CaCl_2$, respectively, and were adjusted to pH 7. The 1-mercapto-6-hexanol (MCH) was obtained from Aldrich. The 1-mercapto-11-undecyl triethylene glycol (denoted PEG−SH) was obtained from Asemblon (Redmond, WA).

DNA Immobilization and Hybridization. Substrates for SPR analysis were SF-10 glass slides coated with 2 nm of Cr followed by 47.5 nm of Au, obtained from Gentel Biosciences (Madison, WI). Substrates for XPS analysis were Si(100) wafers coated with 5 nm of Ti followed by 100 nm of Au, obtained from Platypus Technologies (Madison, WI). Both types of gold surfaces were cleaned with "piranha" solution [70% H_2SO_4, 30% H_2O_2 (30% H_2O_2 in H_2O)] and rinsed thoroughly with deionized water (18.2 MΩ) immediately prior to use. ***Caution!*** *Piranha solution is extremely oxidizing, reacts violently with organics, and should be stored in loosely covered containers to avoid pressure buildup.*

DNA immobilization followed a procedure that yields high surface densities of A*m*−T*n*−P probes:[19] clean gold surfaces were incubated at 35 °C for 20 h with DNA solutions (4 μM total DNA concentration in $CaCl_2$-TE buffer) in silicone isolation wells (four wells per SPR sensor) and covered with a glass slide. After immobilization, each sample was rinsed sequentially with deionized water, NaCl-TE, dilute NaOH, and deionized water. This four-step rinse procedure removes calcium ions and weakly bound DNA. For in situ SPR measurements of DNA immobilization, similar conditions were used, though measurements were limited to 2 h. In order to achieve a surface density comparable to that of the A*m*−T*n*−P15 probes, the 3′ thiol-modified probe, P15−T5−SH, was immobilized in NaCl-TE at room temperature for 2 h. Solutions for hybridization experiments contained 4 μM target DNA in NaCl-TE buffer at room temperature.

Simple DNA arrays with 500 μm × 500 μm gold regions surrounded by a monolayer of PEG−SH were prepared by soaking piranha-cleaned SPR sensors for 20 h in ethanolic 1 mM PEG−SH, rinsing, drying, covering with a mask, and treating for 2 h under a 500 W UV mercury arc lamp equipped with a liquid IR filter.[21] The resulting patterned SPR sensors were rinsed with ethanol and buffer solution prior to DNA probe immobilization.

Surface Plasmon Resonance Analysis Procedure. DNA immobilization and hybridization were quantified in situ using an SPR imaging system (GWC Technologies, Madison, WI). In this system, the gold side of the SPR sensor is in contact with a liquid

(19) Opdahl, A.; Petrovykh, D. Y.; Kimura-Suda, H.; Tarlov, M. J.; Whitman, L. J. *Proc. Natl. Acad. Sci. U.S.A.* **2007**, *104*, 9–14.
(20) Kimura-Suda, H.; Petrovykh, D. Y.; Tarlov, M. J.; Whitman, L. J. *J. Am. Chem. Soc.* **2003**, *125*, 9014–9015.
(21) Zhou, C. Z.; Walker, A. V. *Langmuir* **2006**, *22*, 11420–11425.

Table 1. DNA Probe Coverages and Hybridization Responses

probe name	probe coverage after 2 h, SPR (10^{13} cm^{-2})	probe coverage after 20 h, XPS (10^{13} cm^{-2})	hybrids formed with P15′ (10^{12} cm^{-2})[a]	hybrids formed with T15 (10^{12} cm^{-2})[a]
A15	1.37 ± 0.07	1.34 ± 0.04	<0.2	1.8 ± 0.5
P15	1.09 ± 0.10		1.5 ± 0.2	<0.2
P15−T5−SH	0.82 ± 0.08		2.5 ± 0.3	<0.2
P15−T5−SH + MCH[b]			3.5 ± 0.2	
A15−T5−P15	1.29 ± 0.03	1.90 ± 0.05	3.3 ± 0.3	1.8 ± 0.2

[a] Hybridization experiments shown in Figures 2 and 3. [b] These P15−T5−SH-coated surfaces were treated with a 1 mM MCH solution for 4 min prior to hybridization experiments.

flow cell,[22] while the glass side is index-matched to an equilateral prism. In a fixed observation angle configuration, a polychromatic beam collimated to a diameter of ≈1.5 cm enters the prism, reflects off the sensor, exits through a 794 nm notch filter, and enters a CCD camera.

Quantitative analysis follows established methods for fixed-angle SPR, where for small changes in the refractive index (n), changes in reflected light intensity (ΔI) are proportional to Δn.[23,24] Sensitivity factors (S) that relate Δn to ΔI are determined experimentally for each region of the sensor. DNA surface densities are then calculated using eq 1, where l_d is the decay length of the evanescent wave, n_a and n_s are the refractive indexes of the DNA and the buffer solutions at the analysis wavelength, respectively, ρ_{DNA} is the bulk density of the DNA, and MW_{DNA} is the molecular weight of the DNA. Following Jung et al., l_d, was determined to be approximately 350 nm.[23] We assumed values of DNA density (1.7 g/cm^3) and refractive index (1.7) that are commonly used for SPR quantification.

$$\text{DNA (cm}^{-2}) = \left(\frac{l_d}{2}\right)\left(\frac{\Delta I}{S(n_a - n_s)}\right)\left(\frac{\rho_{DNA} N_A}{MW_{DNA}}\right) \quad (1)$$

The sensitivity factor (S) for each analyzed region of the sensor was calibrated immediately before and after each experiment by measuring changes in reflected light intensity while flowing through the cell NaCl solutions of ionic strength between 0.90 and 1.00 M. Refractive indexes of the calibration solutions were measured using an Abbe refractometer. Calibration using salt solutions yielded comparable results for sensitivity factors to those obtained from ethanol/water mixtures (4−10% ethanol in deionized water). Error bars presented for SPR measurements reflect the standard deviation from replicate samples.

Special consideration was taken to obtain quantitative measurements during the stringency rinse experiments. Prehybridized SPR sensors (hybridized in 1 M NaCl) were rinsed with successively lower ionic strength buffer solutions for 4 min. After each rinse step, a "DNA-free" 1 M NaCl buffer was flowed through the liquid cell and the change in reflected light was recorded. Returning to the original ionic strength buffer solution after each step allows these changes in light intensity to be directly attributed to DNA loss, thus eliminating the need to account for differences in refractive index of the rinse buffers.

X-ray Photoelectron Spectroscopy. Quantitative XPS analysis was used to measure surface densities of DNA probes ex situ for several witness samples, which were prepared similarly to samples used in SPR hybridization measurements (20 h immobilization period). XPS was performed in a system equipped with a monochromatic Al Kα source, a magnetic electron lens, and a hemispherical electron energy analyzer; data were analyzed using previously described methods.[18,19,25] Briefly, normal-emission angle-integrated scans were acquired in Au 4f and 4d, N 1s, P 2p, C 1s, and O 1s regions at 0.36 eV analyzer resolution. The measured peak intensities for the elements from DNA and Au substrates (bare and with DNA films) were analyzed for each sample, assuming a uniform overlayer model that included attenuation of photoelectrons.[19,25] DNA surface densities were calculated from the measured N surface density (amount of substance) and chemical compositions of the deposited DNA probes.[19,25]

RESULTS AND DISCUSSION

The schematic in Figure 1 illustrates the predicted characteristics of DNA strands immobilized on gold using the method evaluated in this work: probe attachment via blocks of (dA), resulting in an approximately L-shaped conformation and systematically controlled surface density of probes. The previous proof-of-principle demonstration of this method relied on ex situ analysis of simplified Am−Tn sequences,[19] for which these characteristics could be inferred from distinct spectroscopic signatures of dA and dT.[18−20,25,26] To evaluate this attachment method for practical probes, which have mixed nucleotide content, we first consider the immobilization and hybridization properties of a 15-nucleotide arbitrary sequence (P15) that is linked to several variants of an Am−Tn− "attachment block" at the 5′ end.

Attachment of ssDNA to Gold via (dA) Blocks. The first evidence of the attachment via (dA) blocks comes from considering the immobilization of a putative "anchoring" block, A15, which on its own produces a saturation surface density of ca. 1.3×10^{13} cm^{-2} (Table 1). The corresponding *nucleotide coverage* of 2.0×10^{14} cm^{-2} is in excellent agreement with previous XPS measurements of shorter A5 and longer A25 oligos at 1.8×10^{14} and 2.2×10^{14} cm^{-2}, respectively.[19,20] The similarity of dA *nucleotide* surface densities for A5, A15, and A25 is an indication of their adsorption on gold in a flat conformation and is consistent

(22) Tamanaha, C. R.; Malito, M. P.; Mulvaney, S. P.; Whitman, L. J. *Lab Chip* **2009**, *9*, 1468–1471.
(23) Jung, L. S.; Campbell, C. T.; Chinowsky, T. M.; Mar, M. N.; Yee, S. S. *Langmuir* **1998**, *14*, 5636–5648.
(24) Shumaker-Parry, J. S.; Campbell, C. T. *Anal. Chem.* **2004**, *76*, 907–917.
(25) Petrovykh, D. Y.; Kimura-Suda, H.; Tarlov, M. J.; Whitman, L. J. *Langmuir* **2004**, *20*, 429–440.
(26) Petrovykh, D. Y.; Pérez-Dieste, V.; Opdahl, A.; Kimura-Suda, H.; Sullivan, J. M.; Tarlov, M. J.; Himpsel, F. J.; Whitman, L. J. *J. Am. Chem. Soc.* **2006**, *128*, 2–3.

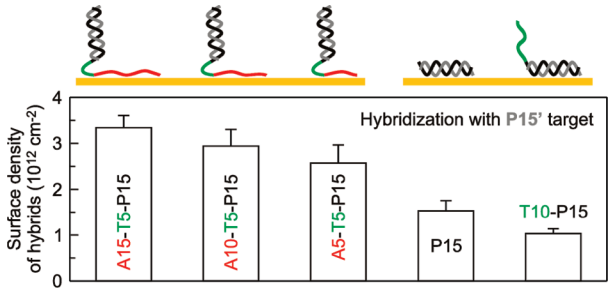

Figure 2. Hybridization activity as a function of immobilized sequence. The P15 probe sequence was immobilized on gold as part of A*m*−T*n*−P15 strands with increasingly longer attachment blocks. These immobilized probes were exposed for ca. 20 min to 4 μM P15′ target in 1 M NaCl-TE. The DNA hybrid density was measured after a posthybridization rinse for ca. 5 min in DNA-free 1 M NaCl-TE; each data point represents an average of measurements made from at least three different SPR sensors.

with the high affinity of dA nucleotides and oligos for gold, the effects of which have been observed by different techniques on a variety of gold surfaces.[4,20,27−30]

A probe strand containing an A15 block, A15−T5−P15, produces surface densities comparable to those of A15 alone (Table 1), indicating that the two oligos occupy a similar footprint on the surface. The much larger *nucleotide coverage* of A15−T5−P15 ($4.6–6.7 \times 10^{14}$ cm^{-2}) then can be achieved only if it adsorbs via about half of the constituent nucleotides, strongly suggesting that A15 acts as the anchoring block for A15−T5−P15.

The main practical advantage of A*m*−T*n*−P15 probes immobilized in L-shaped conformation is the expected increased availability of the P15 sequences for hybridization with solution targets. Indeed, when exposed to the complementary P15′ target, three A*m*−T5−P15 probes in Figure 2 all exhibit hybridization responses enhanced relative to that of the unmodified P15 control. The enhancement is significant for adenine blocks as short as five nucleotides, indicating that the terminal A5 blocks control the conformation of the entire A5−T5−P15 immobilized sequence. Furthermore, the T10−P15 sequence, in which the terminal A5 block of A5−T5−P15 is replaced with T5, exhibits a *reduced* hybridization response relative to the P15 control (Figure 2). The increased hybridization activity of A*m*−T5−P15 probes compared to that of the P15 control (Figure 2), therefore, must result from a mechanism specific to the composition of the A*m*−T5− portion of the probes—a finding consistent with immobilization via the respective A*m* blocks.

Formation and Stability of DNA Hybrids. The strongest evidence for the L-shaped conformation of A*m*−T*n*−P15 probes is provided by the dramatic asymmetries in the hybridization behavior of their two terminals (e.g., A15 vs P15 terminals in A15−T5−P15) and in the stability of the resulting hybrids (Figure 3). These asymmetries are naturally explained by the L-shape model, because the anchoring portion of the sequence (A15 in

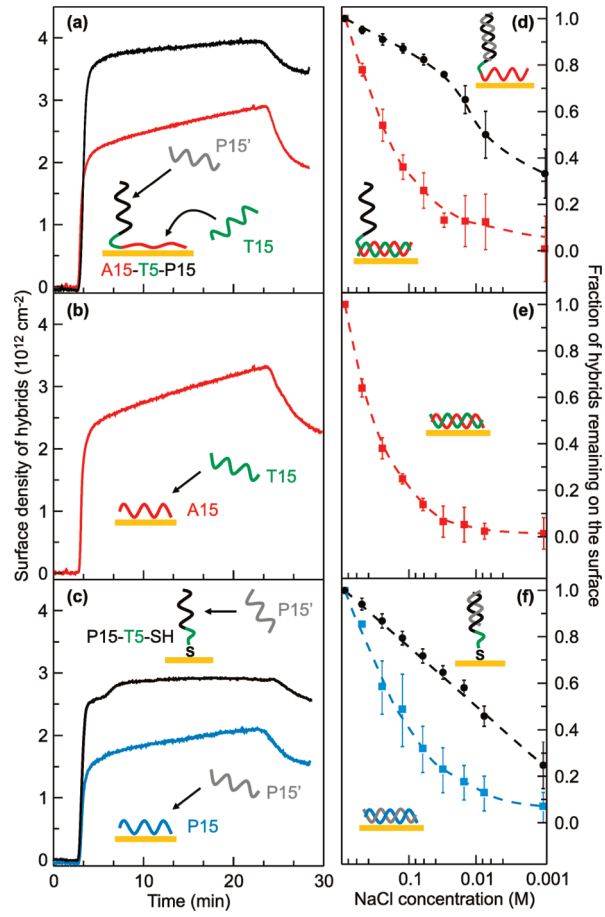

Figure 3. Formation and stability of hybrids formed with probes containing P15 and A15 sequences. Diagrams depict idealized representations of each probe on gold (red = adenine, green = thymine, black/cyan = P15 probe sequence, gray = P15′ target sequence) before (a−c) and after (d−f) hybridization with complementary targets. The line color of the data corresponds with the color used in the corresponding schematic for the probe sequence of the respective hybrids; e.g., in panel a, the black curve corresponds to P15 + P15′ and the red curve to A15 + T15. Hybridization conditions in panels a−c were the same as those in Figure 2; each hybridization signal was recorded for ca. 20 min and followed by a rinse for ca. 5 min in DNA-free 1 M NaCl-TE to remove any weakly bound DNA targets. The stringency rinse profiles (d−f) were obtained by exposing *prehybridized* SPR sensors to solutions of successively lower NaCl concentration and monitoring the number of hybrids remaining on the surface.

Figure 3a) is expected to behave as other fully adsorbed ssDNA probes, whereas the probe portion (P15 in Figure 3a) is expected to behave as other upright probes. These predictions of the L-shape model are verified qualitatively and quantitatively in Figure 3: the hybridization behavior is assessed from a comparison to that of probes immobilized in known conformations (Figure 3, panels b and c), whereas the stability of hybrids is determined from a series of stringency rinses, whereby surfaces with prehybridized probes are exposed to solutions of successively lower ionic strength (Figure 3d−f).

We begin by examining the hybridization behavior of P15 probes immobilized in known conformations (Figure 3c). The unmodified P15 (cyan in Figure 3c) immobilizes at a surface density of 1.1×10^{13} cm^{-2}, which is slightly lower than that of

(27) Anne, A.; Bouchardon, A.; Moiroux, J. *J. Am. Chem. Soc.* **2003**, *125*, 1112–1113.
(28) Demers, L. M.; Östblom, M.; Zhang, H.; Jang, N.-H.; Liedberg, B.; Mirkin, C. A. *J. Am. Chem. Soc.* **2002**, *124*, 11248–11249.
(29) Östblom, M.; Liedberg, B.; Demers, L. M.; Mirkin, C. A. *J. Phys. Chem. B* **2005**, *109*, 15150–15160.
(30) Storhoff, J. J.; Elghanian, R.; Mirkin, C. A.; Letsinger, R. L. *Langmuir* **2002**, *18*, 6666–6670.

A15 (Table 1), i.e., consistent with a fully adsorbed conformation. The hybridization yield with the perfect complement, P15′, is ca. 15% for these directly-adsorbed P15 probes. In contrast, when P15 sequence is specifically immobilized in the form of 3′-thiolated P15−T5−SH probes (black in Figure 3c) at a comparable density of 8.2×10^{12} cm^{-2}, the P15:P15′ hybridization yield doubles to 30%. This higher yield is consistent with the greater accessibility of P15 in the expected end-tethered conformation of thiolated P15−T5−SH probes (diagram in Figure 3c).[31] An even higher yield of >40% is achieved by further increasing the fraction of end-tethered P15−T5−SH probes, which was produced by exposing the surface functionalized with P15−T5−SH to a 1 mM solution of MCH for 5 min prior to hybridization (Table 1).

The stringency rinse data (Figure 3f) show that the hybrids formed by P15 in directly-adsorbed and end-tethered conformations have vastly different stabilities in low ionic strength environments. When surfaces with preformed hybrids are exposed to solutions of successively lower ionic strength, target DNA strands are progressively rinsed away from destabilized hybrids.[17] Control experiments indicate electrostatic destabilization at low ionic strength as the primary factor in reducing the hybrid surface density by these sequential rinse cycles. In contrast, continuous or cyclic rinsing for an extended time *without* changing the ionic strength only removes a much smaller fraction of the hybrids. The density of hybrids remaining after each rinsing step, therefore, forms a stability profile analogous to a thermal melting curve. Although 50% of the hybrids formed with directly-adsorbed P15 are denatured by lowering the NaCl concentration to 100 mM (cyan in Figure 3f), the end-tethered hybrids formed with P15−T5−SH require the NaCl concentration to be lowered to 10 mM for 50% of the hybrids to be denatured (black in Figure 3f). Given that some *hybridization buffers* have ionic strength of ca. 100 mM, these stringency rinses reveal that hybrids formed with directly-adsorbed P15 are extremely unstable. The low hybridization activity and hybrid stability are, therefore, characteristic of P15 strands extensively interacting with surfaces, whereas the high activity and hybrid stability are only exhibited by P15 probes in end-tethered (or similarly upright) conformations.

The above conclusions for unmodified P15 probes are strengthened by the nearly identical behavior of A15 probes (Figure 3, panels b and e). Both directly-adsorbed P15 and A15 probes exhibit similarly low hybridization yields of ca. 15%. The directly-adsorbed A15:T15 hybrids are even less stable than P15:P15′ ones, with ca. 50% removed already at 500 mM concentration of NaCl (Figure 3e).

Hybridization Properties and Conformation of A15−T5−P15. Having established the individual hybridization properties of A15 and P15 in different conformations, we can directly test the accessibility of the 3′ and 5′ ends of A15−T5−P15 probes (Figure 3, panels a and d), thereby verifying their L-shaped conformation. The hybridization signal when the P15 block is targeted by P15′ (black in Figure 3a) is nearly identical to that observed for the end-tethered P15−T5−SH (post-MCH in Table 1). The resulting A15−T5−P15:P15′ hybrids are as stable against stringency rinses as those formed by end-tethered P15−T5−SH (black in Figure 3d). These hybridization and stability properties indicate that the P15 block of A15−T5−P15 does not extensively interact with the gold surface.

In contrast, the hybridization signal between T15 targets and the A15 block (red in Figure 3a) is low, similar to the hybridization response from the directly-adsorbed A15 probes (Figure 3b). The resulting A:T hybrids are as readily removed (red in Figure 3d) as the A:T hybrids formed with A15 probes (Figure 3e), 50% rinsed away already at NaCl concentration of 500 mM NaCl. These hybridization and stability properties indicate that the A15 block of A15−T5−P15 interacts extensively with the gold surface.

Taken together, the hybridization properties of the P15 and A15 blocks in A15−T5−P15 provide strong evidence for the L-shaped conformation of A15−T5−P15, with the A15 block directly adsorbed on the gold surface and the P15 block extending away from the surface (Figure 3a). This conformation adopted by A15−T5−P15 is remarkable, especially considering that the P15 end has 40% adenine content.

Hybridization Efficiency for A*m*−T5−P15 Probes. Quantitatively, the L-shape model predicts that increasing the length *m* of A*m* attachment blocks produces an increase in the average spacing between nearest-neighbor probes (Figure 1, left),[19] resulting in enhanced hybridization efficiency.[17] In agreement with that prediction, the hybridization response in Figure 2 increases with increasing length of A*m* blocks. The T5 sequence used as a *vertical* spacer in A*m*−T5−P15 probes ensures that the P15 probe sequence is always presented far enough from the surface to minimize the effect on hybridization efficiency of any differences between A*m*−T5−P15 probes in terms of their *vertical* spacing from the surface.[32] The systematic change in the hybridization efficiency with the length *m* of the A*m* attachment blocks is then primarily associated with the respective changes in the lateral spacing of the probes.[19,33,34]

The saturation surface density of A15−T5−P15 probes is ca. 1.2×10^{13} cm^{-2}; the corresponding hybridization efficiency is then ca. 25%. Higher efficiencies require further reducing the probe density; however, using adenine blocks that are longer than the probe sequence makes this immobilization method complex and—above ca. 25 nucleotides—rather impractical.

Coimmobilization of A15−T5−P15 and A*k*. To achieve higher hybridization efficiency than the 25% yield measured for the saturated A15−T5−P15 probe surface in Figure 2, we increased the average spacing between probe sequences by coimmobilizing A15−T5−P15 with adenine strands of length *k* (A*k*). During coimmobilization, the smaller A*k* strands compete with A15−T5−P15 probe strands for adsorption sites on gold, ultimately acting as lateral spacers between immobilized probes (Figure 1, right).[19] We use complementary XPS and SPR measurements to confirm that coimmobilized A*k* strands act as lateral spacers and that such coimmobilization increases the hybridization efficiency for A15−T5−P15 probes. The in situ SPR and ex situ XPS impose different constraints on choosing and preparing samples for quantitative measurements; therefore, we primarily use the XPS analysis to determine DNA surface densities on

(31) Wirtz, R.; Walti, C.; Tosch, P.; Pepper, M.; Davies, A. G.; Germishuizen, W. A.; Middelberg, A. P. J. *Langmuir* **2004**, *20*, 1527–1530.
(32) Peeters, S.; Stakenborg, T.; Reekmans, G.; Laureyn, W.; Lagae, L.; Van Aerschot, A.; Van Ranst, M. *Biosens. Bioelectron.* **2008**, *24*, 72–77.
(33) Zu, Y. B.; Gao, Z. Q. *Anal. Chem.* **2009**, *81*, 8523–8528.
(34) Hurst, S. J.; Lytton-Jean, A. K. R.; Mirkin, C. A. *Anal. Chem.* **2006**, *78*, 8313–8318.

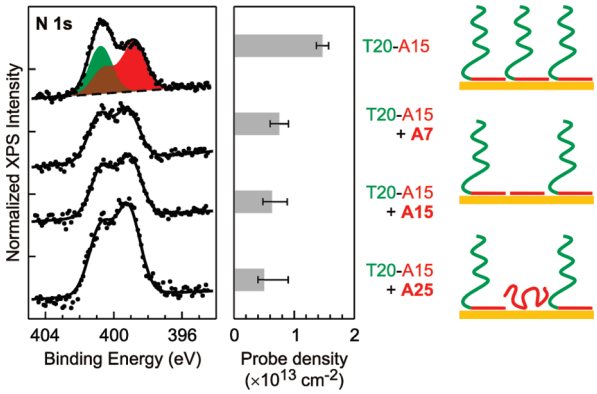

Figure 4. XPS data and surface densities for A15−T20 model probes coimmobilized on gold with adenine lateral spacers. Clean gold surfaces were incubated at 35 °C for 20 h in $CaCl_2$-TE buffer with the total concentration of A15−T20 and A*k* (*k* = 7, 15, 25) of 4 μM; samples were then rinsed sequentially with water, NaCl-TE, dilute NaOH, and water. In the A15−T20 spectrum (top), the characteristic envelopes for thymine and adenine are shaded in green and red, respectively. Error bars indicate the combined uncertainty of measurements (ca. 10%) and of data deconvolution, the latter being responsible for asymmetric uncertainties.

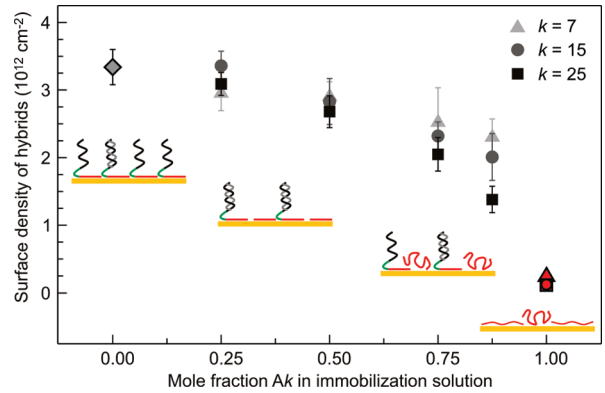

Figure 5. Surface density of P15:P15′ hybrids formed by A15−T5−P15 probes coimmobilized with A*k* lateral spacers on gold surfaces. The total concentration of A15−T5−P15 and A*k* (*k* = 7, 15, 25) during coimmobilization was 4 μM. Hybridization conditions were identical to those used in Figure 2. Each surface density of hybrids (after a posthybridization rinse) is the average from measurements on at least three different SPR sensors. The data for limiting cases of no lateral spacers (A*k* fraction of 0) and no probes (A*k* fraction of 1) are indicated, respectively, by a different symbol (diamond) and color (red).

samples for which SPR does not provide an unambiguous measurement. A previous systematic comparison has found good agreement between DNA surface densities determined by SPR and XPS.[7]

Model A15−T20 "probes", which have the same length and A15 attachment block as the A15−T5−P15 sequence, were used to provide a quantitative model for measuring surface densities of probes ex situ.[19] The *saturation* surface density of A15−T20 "probes" can be determined from XPS data (Figure 4, top) using the method developed in ref 19. For surfaces prepared with A*k* lateral spacers, the deconvolution of N 1s spectra is complex, because both A15−T20 probes and A*k* spacers contribute to the characteristic spectral envelope of adenine (shaded red in Figure 4, top). Qualitatively, the raw data in Figure 4 show that the intensity at ca. 401 eV binding energy (BE) decreases as the length of A*k* increases, suggesting a decreasing density of T20 "probe" sequences.[18,19,25] In addition, the characteristic adenine peak at ca. 399 eV BE remains approximately the same for A7 and A15 spacers and increases for A25 spacers. The behavior of short spacers is consistent with the nearly constant coverage of adenine nucleotides that underpins the L-shape model (Figure 1).[19] The increased normalized N 1s intensity observed for A25 spacers indicates an increased coverage of adenine nucleotides, most likely achieved through coils or loops (bottom schematic in Figure 4). Self-consistently quantified surface densities of probes are shown in Figure 4. The observed changes in probe surface densities are consistent with previous FT-IR measurements for similar model A10−T25 "probes" coimmobilized with A10 and A25 lateral spacers.[19]

The set of SPR measurements summarized in Figure 5 quantitatively examines the effect on hybridization efficiency of the two main adjustable parameters of coimmobilization of A15−T5−P15 with A*k*: the length, *k*, of the A*k* and the relative fraction of A*k* in immobilization solution. Increasing *k* increases the surface footprint of each lateral spacer A*k*, thus leading to increased average distance, *d*, between A15−T5−P15 probes (Figure 1, right). Increasing the fraction of A*k* in immobilization solution increases the relative fraction of A*k* in the mixed layer, thus also increasing the average distance between A15−T5−P15 probes. Immobilization conditions for the mixed layers in Figure 5 were the same as those used to prepare saturated A15−T5−P15 surfaces in Figures 2 and 3.

The data in Figure 5 show that hybridization of P15′ with mixed A15−T5−P15/A*k* surfaces results in a systematic variation of the hybridization response with both length and concentration of A*k*. The hybridization response is $>3.0 \times 10^{12}$ cm^{-2} when the fraction of A*k* in the immobilization solution is <0.25, for all lengths A*k*. Above 0.25 mole fraction of A*k*, the hybridization response trends lower as either *k* or the fraction of A*k* present during immobilization is increased. For films prepared with 0.25 mole fraction A*k*, the surface density of A15−T5−P15 is lower than that in the pure probe film, as suggested by the model data in Figure 4. The nearly identical hybridization response of the former indicates that the 0.25 mole fraction A*k* surfaces produce higher hybridization yields than does the saturated A15−T5−P15 film (Table 1). For surfaces prepared using 0.50 mole fraction A*k*, the reduction of the hybridization response is marginal, for all lengths of *k*. Given the surface density data from the model 0.50 mole fraction A15−T20/A*k* mixed surfaces in Figure 4, the hybridization yield of the 0.50 mole fraction A15−T5−P15/A*k* surfaces in Figure 5 at least doubles from that of A15−T5−P15, reaching values >50%, in agreement with other measurements of optimized DNA hybridization on surfaces.[7]

In qualitative agreement with traditional methods of optimizing DNA−SH surface densities using dilution by small organic thiols, once the probe coverage decreases significantly, the hybridization response also decreases. For the films prepared with A*k* mole fractions >0.50, the A15−T5−P15 density drops to the point where the hybridization signal becomes limited by the number of P15 probes on the surface. In practical measurements, maximizing both hybridization yield and hybridization signal is desirable, suggesting optimal combination of parameters from Figure 5 as A*k* length of 15 or 25 and solution fraction of 0.25.

Reproducibility and Nonspecific Adsorption. Incorporating Am−Tn− at the end of DNA probes as a means to immobilize them onto gold surfaces provides a simple and practical method of controlling the surface density and conformation of DNA probes. Most importantly, since the method relies on saturation densities, the resulting immobilization is highly reproducible. For example, the relative standard deviation of <10% observed for hybridization with A15−T5−P15 probes (Figure 5) is notably low for hybridization data averaged from five different SPR sensors prepared on different days. In addition, the data in Table 1 and Figure 5 show that gold surfaces coated with adenine oligos (A7, A15, or A25) resist nonspecific adsorption of DNA during hybridization. The observed nonfouling behavior in the presence of DNA hybridization solutions is particularly important, because it indicates that nonfouling properties will be maintained even for surfaces prepared to have very low probe densities, as may be desirable in applications that require addressing individual DNA probes independently.

The exception to the resistance of adenine-coated surfaces against unwanted DNA adsorption is their ability to specifically interact with thymine targets (Figure 3b). This interaction, however, is relatively low yielding and weak, evidenced by the hybridization and stringency rinse data (Figure 3, panels d and e). In fact, one of the results in Table 1 and Figure 3 is a measurement of the hybridization activity of directly-adsorbed DNA. Though the hybridization activities of end-tethered, upright DNA probes are well-characterized, quantitative reports for directly-adsorbed probes are difficult to find in the literature, despite their widespread practical use, e.g., in older versions of inkjet printed DNA microarrays.[2] Figure 3 suggests an approximately 50% reduction in hybridization efficiency for directly-adsorbed DNA compared to that for upright DNA probes. Such reduction is consistent with a recent study by Gong et al., which measured hybridization properties for DNA−SH probes while adjusting their density and conformation by displacement with mercaptoundecanol (MCU).[7] Using a similar 1 M NaCl-TE hybridization buffer, Gong et al. reported an approximate doubling of the hybridization signal after backfilling with MCU for <1 h.[7] Complementary measurements confirmed that short MCU treatments dramatically reduced the fraction of the probes directly interacting with the gold surface, with only a small reduction in probe coverage.[6] The combined results of refs 6 and 7 thus also suggest that directly-adsorbed DNA probes are roughly half as active toward hybridization as upright probes in 1 M NaCl. A similar reduction of hybridization activity was also reported for DNA probes immobilized on gold via thiols incorporated in the middle rather than at the end of a probe sequence.[31]

We observed that the hybridization activity of directly-adsorbed DNA is much more sensitive to ionic strength than is the hybridization activity of upright probes. For example, when 0.25 M NaCl-TE buffer was used in the hybridization step (data not shown), we measured a greater than 5-fold difference in hybridization activities of the P15 and A15 blocks of A15−T5−P15 (1.9×10^{12} vs 3.5×10^{11} cm^{-2}, respectively). This observation suggests that unwanted specific interactions between directly-adsorbed adenine and thymine targets can be minimized by either hybridizing in a buffer with NaCl concentration <0.25 M or by performing a brief stringency rinse after hybridizing (Figure 3e).

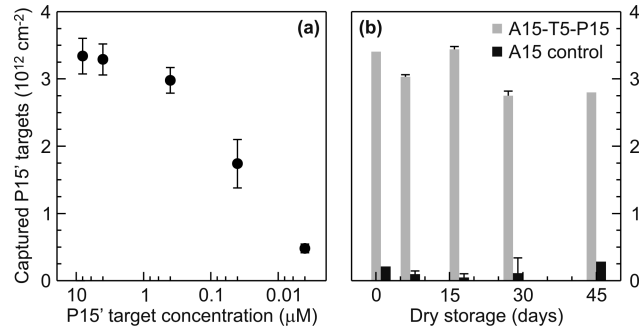

Figure 6. Practical aspects of A15−T5−P15 probe modified surfaces. (a) Dependence of hybridization signal on target DNA abundance. Hybridization was measured for saturated A15−T5−P15 surfaces using P15′ concentrations between 4 μM and 4 nM and other conditions identical to those in Figure 2. (b) Shelf life of A15−T5−P15 probes on surfaces. Gray bars indicate surface densities of P15:P15′ hybrids measured on A15−T5−P15 surfaces rehydrated after dry storage in a sealed container; black bars indicate nonspecific adsorption of P15 onto stored and rehydrated A15 surfaces. Hybridization conditions were identical to those in Figure 2.

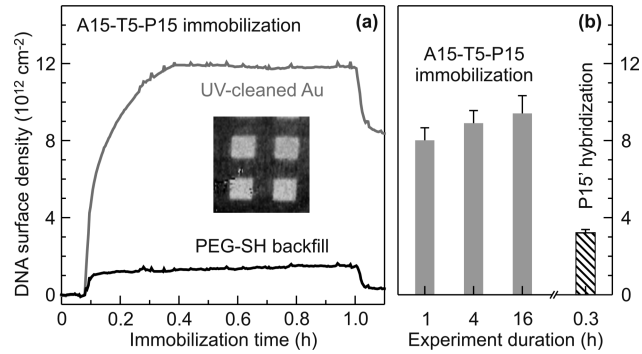

Figure 7. Immobilization and hybridization data for A15−T5−P15 on a photopatterned SPR sensor. The A15−T5−P15 probes were selectively immobilized onto 500 μm × 500 μm gold regions surrounded by PEG−SH (graphs in panel a, gray bars in panel b) and hybridized with P15′ targets (hatched bar in panel b). Immobilization and hybridization conditions were identical to those in Figure 2.

Stability. Probe surfaces prepared by this method are sufficiently stable to be readily regenerated by rinsing with dilute NaOH after hybridization. A sensor functionalized with A15−T5−P15, for example, showed <3% change in hybridization signal during six sequential hybridization/regeneration cycles. To test shelf life, we prepared several SPR sensors with A15−T5−P15 and A15 regions and tested them by hybridization with P15′ over several weeks of dry storage in sealed plastic containers. The results in Figure 6b show no significant changes in either hybridization signal from A15−T5−P15 regions (gray bars) or resistance to nonspecific adsorption of P15′ in A15 regions (black bars) over a period of 42 days.

Dose−Response Measurements. Reproducibly immobilizing DNA probes to produce hybridization responses that can be quantitatively correlated to abundances was an important motivation for this work. Figure 6a shows the hybridization response of A15−T5−P15 probes as a function of the concentration of P15′ targets. At P15′ concentrations greater that ca. 1 μM the hybridization response is saturated at 3.3×10^{12} cm^{-2}. Target concentration below 1 μM is likely insufficient to saturate the sensor response during the ca. 20 min measurement, so the

hybridization response decreases as the P15′ abundance drops below 1 μM. The detection limit of ca. 4 nM corresponds to a dynamic range of ca. 2 decades in measuring target DNA *abundances*. Although this particular assay has not been optimized to lower the detection limit, the 4 nM value is comparable to those reported from SPR measurements for other DNA immobilization methods, suggesting that instrument performance limits the ultimate sensitivity.[16,17]

Patterning. Practical array fabrication using gold often requires immobilizing onto UV-cleaned gold, i.e., after a cleaning treatment that is less aggressive than piranha solution. To test attachment via (dA) blocks to such gold surfaces, we created a DNA sensor in a simple array format. Patterned surfaces were created by exposing a gold surface precoated with PEG−SH to UV light from a mercury arc lamp through a mask. This exposure produced an array of 500 μm × 500 μm squares of UV-cleaned gold separated by PEG−SH regions (Figure 7a, inset). The initial measurements (Figure 7a) confirmed that A15−T5−P15 probes immobilize selectively in the exposed gold regions of the array. Quantitatively, the saturation coverages of A15−T5−P15 (9.4×10^{12} cm^{-2}) were lower than those achieved on piranha-cleaned gold, suggesting that residual contamination is left on gold after UV patterning, but this contamination does not prevent the majority of A15−T5−P15 probes from immobilization. The corresponding hybridization response of 3.2×10^{12} cm^{-2} favorably compares with the values from Table 1 and Figure 2, indicating that the A15−T5−P15 probes maintain the L-shaped conformation and high hybridization activity, even when immobilized on gold surfaces that were cleaned by a UV treatment.

CONCLUSION

We have demonstrated that controlled and efficient hybridization can be achieved with DNA capture probes immobilized solely through preferential DNA-substrate interactions. All of the data from the series of experiments presented here support a model where competitive nucleotide-surface interactions control the conformation and surface density of the immobilized DNA, with the A*m* block of A*m*−T*n*−P DNA strands preferentially adsorbed on gold, presenting the probe sequence, P, in a conformation accessible for efficient hybridization. The successful immobilization of the mixed nucleotide P15 sequence via (dA) block attachment indicates that this method should be generally applicable to realistic DNA sequences. A wide range of probe-to-probe spacing can be realized by coimmobilizing A*m*−T*n*−P with unmodified A*k* lateral spacers, providing a means to prepare surfaces with tunable hybridization response and yield. This preparation method offers many desirable properties for practical biosensors, including simplicity in fabrication, highly reproducible hybridization, and long-term stability. More generally, DNA with many types of functional modifications, such as biotin and *N*-hydroxysuccinimide (NHS), can be readily obtained from vendors. Incorporating these modifications at the end of an A*m*−T*n*−X (X = biotin or NHS) would extend the method described here as a simple means to produce biotin- or NHS-functionalized surfaces having highly tunable and reproducible properties.

ACKNOWLEDGMENT

Research at UW−La Crosse was supported by an award from Research Corporation. Research at the Naval Research Laboratory (NRL) was supported by the Office of Naval Research and the Air Force Office of Scientific Research. A.O. thanks B. P. Nelson for advice on SPR measurements. D.Y.P. thanks T. D. Clark (NRL) for stimulating discussions of DNA properties.

Received for review December 4, 2009. Accepted January 28, 2010.

AC902765G